J. Biomechanics Vol. 13, pp. 701–715.

0021-9290/80/0801-0701 $02.00/0

MECHANISMS OF FEMORAL FRACTURE*

DAVID C. VIANO
Biomedical Science Department, General Motors Research Laboratories, Warren, MI 48090, U.S.A.
and
RICHARD L. STALNAKER
Highway Safety Research Institute, University of Michigan, Ann Arbor, MI 48109, U.S.A.

Abstract – Mechanisms of femoral fracture of the condyles and shaft were experimentally investigated through controlled knee impact of denuded femurs in six human cadavers. High-speed movies recorded knee joint compression, femoral displacements and deformation, and fracture initiation. Fracture initiated at 10.6 ± 2.7 kN knee load after 1.3 ± 0.1 cm of knee joint compression for a 10.1 kg rigid impact at 13.2 ± 1.4 m/s. Interestingly, fracture occurred 0.5 ms–1.5 ms after the peak in applied knee load of 18.3 ± 6.9 kN, probably because a significant portion of the load is developed by inertial accelerations displacing the femur and coupled masses. Axial strain measurements at the femoral midshaft showed increasing anteroposterior bending and compressional deformations until the initiation of observed fracture. The kinematics of the observed fracture and the midshaft deformational strains indicate that fracture is predominantly due to tensile strain from anteroposterior bending of the femoral shaft or patellar wedging of the condyles.

INTRODUCTION

Response and trauma associated with axial knee impact has been the subject of numerous experimental investigations (Cooke and Nagel, 1969; Horsch and Patrick, 1976; Kramer *et al.*, 1973; Kroell *et al.*, 1976a; Kulowski, 1964; Lister and Wall, 1970; Melvin and Stalnaker, 1975 and 1976; Patrick *et al.*, 1965; and Powell *et al.*, 1974 and 1975) and analytical studies (Advani *et al.*, 1975; King *et al.*, 1973; Koch, 1917; and Viano and Khalil, 1976b and 1976c). Most of this research has been aimed at improving occupant protection in automobile accidents. However, the experimental work with human cadavers has provided only limited information on mechanisms of trauma initiation, since the major effort has been directed at the need for a force tolerance level for femoral injury. A peak force injury criterion was needed because anthropomorphic test dummies, used in automotive crash testing, measure axial femur force and a criterion compatible with current test dummies would be used to assess automotive crash protection. Thus, emphasis was naturally directed toward force. However, there has been a continuing need to fundamentally address the underlying mechanisms of femoral fracture and confounding factors.

Early studies (Patrick *et al.*, 1965) with fully articulated embalmed cadavers indicated that a femur force injury threshold of 6.2 kN (1400 lb) was a 'reasonably conservative' tolerance level for human protection. Additional investigation of this experimental data led to a revised tolerance level of 8.7 kN (1950 lb), which was 'not unreasonable" for the evaluation of occupant protection. However, other studies (Melvin and Stalnaker, 1975 and 1976; and Powell *et al.*, 1974 and 1975) with embalmed and unembalmed cadaver specimens demonstrated that substantially higher knee impact loads did not produce femoral fracture.

A wide variation in peak applied force was observed in these studies with and without the occurrence of femur fracture (See review by Viano, 1977a). In many cases the experimental protocol provided a dominant influence on the range of experimental outcomes. The most recent axial knee impact tests (Melvin and Stalnaker, 1975 and 1976; and Powell *et al.*, 1974 and 1975) have been conducted with a relatively lightweight striker mass (10.1–15.6 kg) and high impact velocity (6.3–23.2 m/s). Conceptually, this impact involves different inertial loading conditions than might be expected in an automobile accident. In the field accident, the occupant accelerates forward and strikes the automotive interior; whereas, in the component tests an impactor mass accelerates against a stationary specimen. The different impact characteristics produce a rather short duration contact exposure (5–40 ms) in laboratory experiments, as opposed to longer duration loads (50–150 ms) in field accident simulations.

Structural analysis of the femur by finite element techniques (Viano and Khalil, 1976b and 1976c) has shown that the femur responds as a 'column-like' structure under compressive knee loads. Because the natural frequency of the lowest bending mode of the femur falls between 100 and 200 Hz (Melvin and Stalnaker, 1975 and 1976) the dynamic load level at fracture was shown to depend on the primary duration of the impact. Both model and available experimental data substantiated this time-dependent peak fracture load phenomenon for impact durations below 20 ms

* *Received* 6 *September* 1978; *in revised form* 16 *October* 1979.

(Viano and Khalil, 1976c and Viano, 1977a). In fact, a near doubling of the allowable femur load occurs as the duration of the primary impact pulse decreases from 20 ms (quasistatic response) to 10 ms (structural response).

Unfortunately, even this discovery was not sufficient to explain the large variation in peak force observed in both fracture and non-fracture producing cadaver impact experiments. It was clear that several confounding influences were probably contributing to the variation in response. The human cadavers were generally aged, typically in poor health prior to their demise, and frequently in an advanced state of osteoporosis. Osteoporosis has been shown to significantly degrade the skeletal strength of long bones in axial knee impact (Melvin and Stalnaker, 1976). Since age and pathology may reduce the skeletal strength by a factor of three, some degree of explanation is available for the large variation in peak force associated with experimental femur fracture. However, several researchers have recognized that peak force alone is not a sufficient measure of potential fracture (Cooke and Nagel, 1969; McElhaney and Byars, 1966; Melvin and Stalnaker, 1976; and Viano 1977a). So that parameters, such as available energy or momentum, have been proposed as additional factors influencing tolerance.

Recent investigations have shown that human injury is generally not highly correlated with measures of applied force (Goldsmith, 1972; Kroell, 1976b; and Viano, 1978b) because dynamic applied force produces two biomechanical reactions: (1) direct inertial acceleration of body regions – thus causing whole segment *displacements*, and (2) direct compression and shear of body regions – thus causing localized *deformations*. Unfortunately, both reactions occur simultaneously and constitute differing portions of the total applied load. In most cases, the induced deformation causes the injury, while the early force peak is predominantly an inertial reaction – not causally associated with injury production. Based on this observation, an experimental investigation was initiated into the underlying biomechanics and parametric dependencies associated with knee impact induced femoral fracture.

Since the experiments conducted by Melvin and Stalnaker (1975 and 1976) at the University of Michigan resulted in the most comprehensive cadaver knee impact data available at this time, additional cadaver tests were recently conducted (Stalnaker *et al.*, 1977) at the University of Michigan using the same impact protocol. However, a more extensive experimental methodology was employed to study additional biomechanical responses. In these tests, the soft tissue was removed from the specimen's femur so that the kinematics (Viano, 1977b) of structural deformations and displacements of the skeleton could be followed during the impact. This was accomplished by high-speed photography of the denuded femoral response. Three strain gages (Melvin *et al.*, 1975 and Powell *et al.*, 1975) were attached at the femoral midsection for subsequent analysis of the midshaft bending and compression. Pelvic acceleration was also monitored. All of this effort was directed at collecting a more complete description of the biomechanical responses associated with axial knee impact induced fracture.

Excluded from this investigation was analysis of potential knee joint injury through either ligamentous tears/avulsions (Drucker and Wynne, 1975; Kennedy and Fowler, 1971; Kennedy *et al.*, 1974; Noyes *et al.*, 1974, 1976, and 1977; O'Donnel *et al.*, 1977; and Trickey, 1968), subchrondral bone injury (Radin *et al.*, 1971 and 1973) or articular cartilage damage (Repo and Finlay, 1977). This is not to preclude the potential significance of soft tissue injury in the field situation, but rather to concentrate this limited study on the skeletal performance and mechanisms of femoral fracture. Certainly, some soft tissue effects were observed in this study. Other features of knee joint performance during lower extremity impact are covered in more detail in a companion effort (Viano *et al.*, 1978a).

METHODOLOGY

Cadavers were obtained through a willed-body program administered by the Department of Anatomy, School of Medicine at the University of Michigan. The specimens were tested at the Highway Safety Research Institute of the University of Michigan under a General Motors Research Laboratories' contract. In these experiments, the flesh on the right and left femur was carefully removed from the bone from the proximal epiphysis to the femoral condyles of the knee joint (refer to Fig. 1a–c). Caution was exercised so that all ligaments of the knee joint were left intact. Only muscle was removed from the femoral and anterior patellar surfaces. This precluded the complete exposure of the posterior and some of the lateral aspects of the femoral condyles so that the structural integrity of the knee joint, especially the collateral ligamentous attachment, was not destroyed.

The femoral midshaft was selected for strain gaging. The region was thoroughly cleaned of soft tissue and sanded smooth with 320 grit wet abrasive paper, while flushing with 99% ethyl alcohol. Three uniaxial Micro-Measurement type EA-13-250BG-120 strain gages were applied along the axis of the femur at three circumferential midshaft locations (refer to footnote, Table 2). Gages and cable relief tabs were bonded to the bone with Micro-Measurement's M-Bond 100 (methyl-2-cyanoacrylate) adhesive. Cables were then secured to the proximal femur shaft by nylon ties for additional gage relief. The denuded femur was then marked with 2 mm dia. ink dot targets so that subsequent high-speed movie analysis could be performed to define gross skeletal motion, knee-joint compression, and structural deformational response of the femur during impact. The entire bone surface was then covered with a thin coating of petroleum jelly to reduce the potential loss of moisture.

Fig. 1a. Lateral view kinematics of the denuded femur (3R20693 N/L) for a rigid axial knee impact. Note the increase in anteroposterior bending in the 1 ms and 3 ms sequence and fracture initiation on the anterior surface of the femoral midshaft.

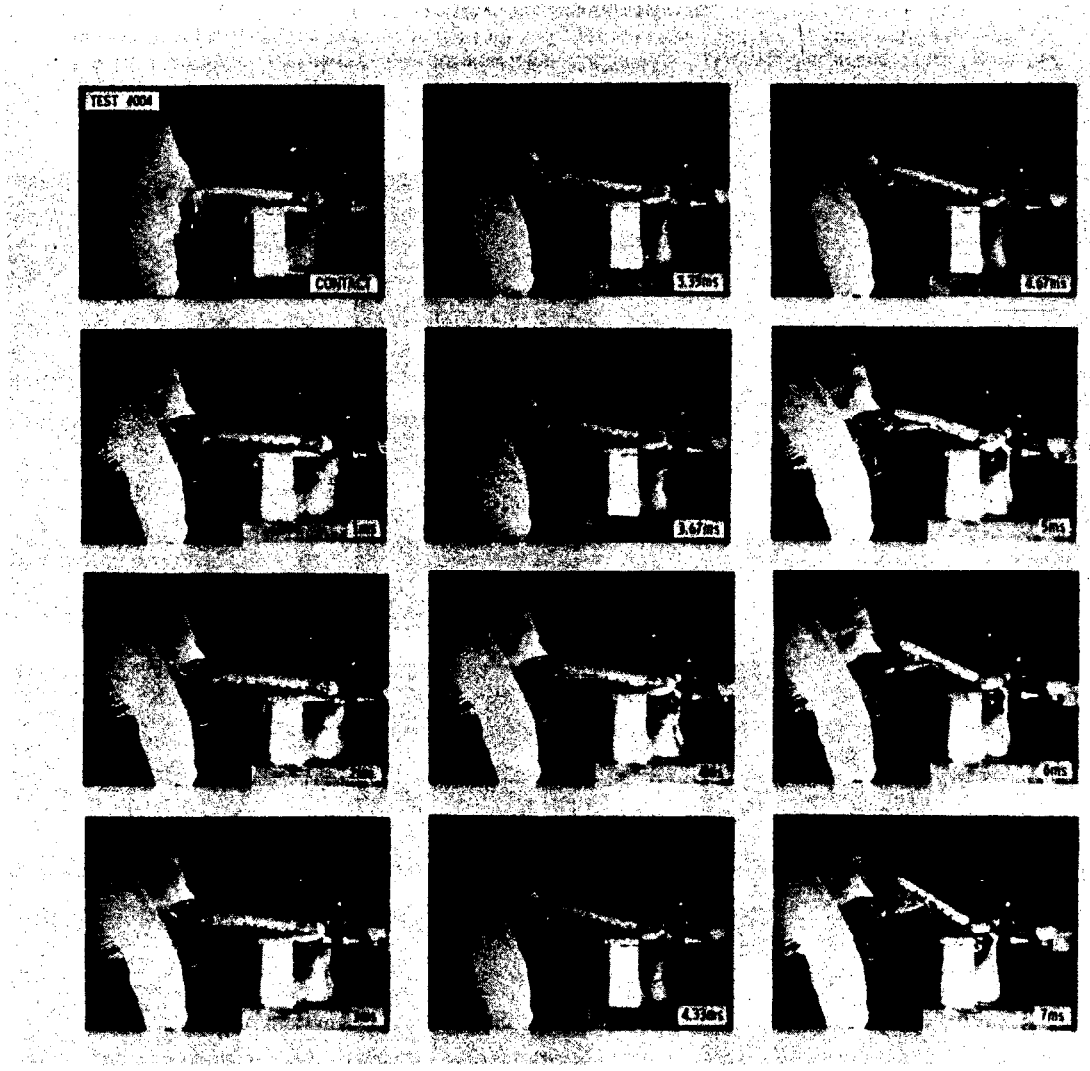

Fig. 1b. Lateral view kinematics of the denuded femur (4R20693 N/R) for a rigid axial knee impact. Fracture initiation is again on the anterior surface of the femoral midshaft.

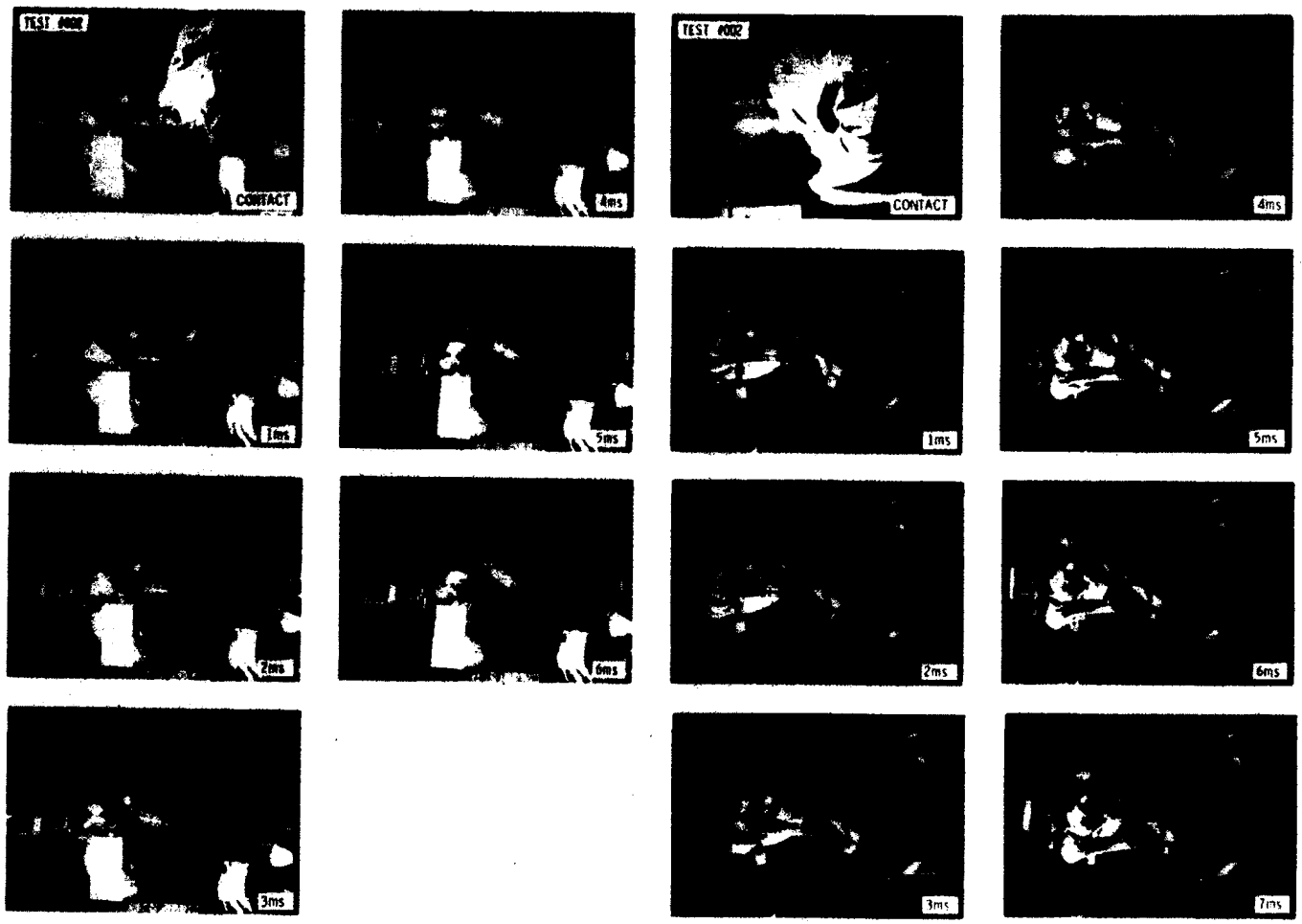

Fig. 1c. Lateral and anterior view kinematics of the denuded femur (2R20690 *A/L*) for a rigid axial knee impact. Note the *AP* condylar bending (lateral view) and patellar wedging of the condyles (anterior view) during fracture.

Each strain gage was connected to a Honeywell Accudata 120 through an Accudata 105 for signal conditioning. A triaxial acceleration package was fixed to a pelvic mount, which was rigidly attached to the posterior-superior iliac spines of the specimen. These orthogonal accelerometers (Endevco Model 2264/2000), which measured midsaggital pelvic acceleration, were also connected to the Honeywell Accudata 120 and 105. The orientation of the accelerometer package in the laboratory and specimen coordinate system was measured and recorded. The impactor force and acceleration, camera synchronization flash signal, femur strains, and pelvic accelerations were recorded on a Honeywell 7600 FM tape recorder.

Prior to impact, the cadaver was placed on a balanced wooden block. The legs were supported on the inferior–posterior surface of the femur by a half-inch diameter steel rod loosely supported at the ends. The cadaver was positioned so the femur shaft was aligned along the axis of the impact. The lower leg was then pulled back (Melvin and Stalnaker, 1975 and 1976) so that the patella was in line with the impactor axis. The cadaver's upper torso was also tipped back allowing an overhead camera view of the anterior aspect of the knee-joint and femur.

Two high-speed cameras photographed the impact phenomena: a Hycam (3000 fps) for the lateral aspects of the response and a Photosonics (1000 fps) for the anterior. A timing generator provided exposure marks on the edge of the film at a constant interval to verify the actual film framing rate. In all tests the framing rate was constant ($\pm 5\%$) as specified during the impact. Knee contact was sensed by closure of a normally open circuit composed of parallel aluminum foil strips attached to the cadaver's knee. A transverse strip on the face of the impactor completed the circuit on knee contact. Closure of the circuit also produced a rapid flash in the field of camera view and a simultaneous voltage spike on a tape recorded channel. This procedure ensured synchronization of the tape digitized data (at 0.10 ms intervals) to lateral view film analyzed data (at 0.33 ms intervals). Thus, time zero between the two measurement procedures was accurate to within ± 0.17 ms, a single frame of film. Digitization of femoral kinematics from the high-speed films provided a resolution of 4 points/mm of actual motion. However, the physical size of targets on the impactor and femur produced a practical resolution of displacement to within ± 1 mm.

Using the synchronized optical flash and taped voltage spike at impactor-knee contact, photo-analyzed displacements and deformation of the femur were coherently compared with tape recorded force, strain, and acceleration histories. In particular, the temporal history after knee contact of the axial motion of the impactor and the planar motion of a point on the femoral midsection were recorded from the high-speed movie films. These measurements were used to compute the compressive deformation of the knee-joint, i.e., the tissue between the impactor and femoral condyles. The deformational responses were compared with the applied force. The first sign of fracture on the surface of the exposed femur was also noted, as well as the apparent mechanism of the induced trauma.

Impact was administered with a pneumatic testing machine specifically constructed for high-speed impact studies (Melvin and Stalnaker, 1975 and 1976). The impactor consisted of an air reservoir and a ground/honed cylinder with two carefully fitted pistons. The transfer piston, which was propelled by compressed air, delivered its momentum to the impact piston. A striker surface and load cell were attached to the impact piston. This piston was allowed to travel up to twenty-five centimeters and then its motion was arrested by an inversion tube, which absorbed the remaining kinetic energy. The desired impactor stroke was controlled by the initial positioning of the impact piston with respect to the inversion tube. The impactor velocity was controlled by reservoir pressure and the ratio of the mass of the transfer and impact piston. The load cell was a Kistler 904A piezoelectric load washer with a Kistler 805A piezoelectric accelerometer mounted internally for inertial compensation, i.e., adjusting the load cell force measurement for the effect of the striker acceleration of the mass between the load measuring cell and the impact surface. The impact-piston and load-cell striker assembly weighed 10.1 kg (22.2 lb). The rigid flat striker surface was 15.2 cm (6 in.) in diameter. The striker was either uncovered or interfaced with energy absorbing material: (1) lightly padded (LP) with 2.5 cm Ensolite or (2) thickly padded (TP) with 2.5 cm Ensolite plus 5.0 cm Hexcell.

Six human cadavers were utilized in this test series which included thirteen axial knee impacts (Table 1). The specimens were typically aged and generally exhibited some degree of geronological pathology. Several specimens were sufficiently osteoporotic that a classification of 'abnormal' was attached to their test identification. Subsequent to the cadaver test, a careful dissection of the hip and knee joint was performed to identify the injuries (refer specifically to Stalnaker *et al.*, 1977). When gross trauma was observed, it was classified according to the American Association for Automotive Medicine's Abbreviated Injury Scale, AIS. The femurs were also characterized by a set of osteometric measurements made at autopsy. The diameter in the anterior–posterior and in the lateral–medial directions, as well as the circumference was recorded at the femoral midsection. Other measurements included femoral and tissue weights plus whole-body anthropometry and specimen characteristics.

The femur was then sectioned at the site of strain gaging and a photograph was made of the cross-sectional geometry and gage locations for analyses of geometric properties at the gaged section. This enabled computation of the bending and compressive strain response at the midfemur. The computation was accomplished by determination of the principal centroidal axes system of the midshaft cross section (Viano *et al.*, 1976a) and a simple matrix operation

Table 1. Cadaver and lower extremity characteristics

Experimental condition*	Sex	Specimen characteristics: Age (yr)	Weight (kg)	Height (m)	Cause of death	Femur: Weight (kg)	Length (cm)	Excised Tissue weight (kg)	Femur osteometry at midshaft: Lat. diam. (cm)	AP diam. (cm)	Circ. (cm)
1R20690A/R	F	54	99.6	1.70	Breast Cancer	0.76	42.3	5.43	3.4	2.8	9.4
2R20690A/L						0.73	42.2	6.10	3.3	3.0	10.2
3R20693N/L	F	51	75.6	1.53	Cardiac Arrhythmia	0.57	42.0	3.70	2.4	2.6	7.9
4R20693N/R						0.58	41.9	3.86	2.3	2.8	8.3
5LP20698N/R	M	74	89.7	1.66	Myocardial Infarction	0.70	44.0	3.59	2.8	2.6	9.2
6LP20698N/L						0.68	43.9	3.59	2.7	2.8	9.1
7R20709N/L	M	73	69.9	1.72	Pulmonary Artery	0.97	49.6	3.92	3.1	3.2	10.3
8R20709N/R					Obstruction	0.96	49.2	4.00	3.1	3.2	10.3
9TP20703N/R	M	61	53.2	1.83	Respiratory Failure	1.14	51.4	2.29	3.2	3.7	11.5
10TP20703N/L						1.18	51.2	2.33	3.4	3.9	12.9
11TP20703N/R											
12TP20711A/R	M	65	61.8	1.59	Myocardial Infarction	0.59	44.0	3.92	2.6	2.5	8.8
13TP20711A/L						0.58	43.6	3.69	2.6	2.6	8.5
		63.0 (±9.5)	75.0 (±17.3)	1.67 (±0.10)		0.79 (±0.22)	45.4 (±3.8)	3.87 (±1.07)	2.9 (±0.4)	3.0 (±0.4)	9.7 (±1.4)

* 1R20690A/R
- 1: Test number
- R: Impactor interface: rigid; lightly or thickly padded
- 20690: Specimen ID number
- A: Bone condition: reasonably normal or abnormal
- R: Impacted leg: Right or Left

(refer to footnote, Table 2) on the measured strains ($\varepsilon_1, \varepsilon_2, \varepsilon_3$) based on strain gage location. The axial compression–elongation (ε_A), anterior–posterior bending (ε_{AP}) and lateral-medial bending (ε_L) responses about the principle centroidal axes provide the major components of axial strain. The computed strains are considered more useful for comparison of injury occurrences and biomechanical responses. In this fashion, the strain at a particular x, y location at the gaged section is composed of the sum of three independent strain responses [$\varepsilon_{x,y}(t) = \varepsilon_A(t) + y\varepsilon_{AP}(t) + x\varepsilon_L(t)$]. In addition, fundamental mechanics of induced compression and bending due to a primarily axial load could be studied in regard to the various modes of femoral fracture.

AXIAL KNEE IMPACTS

The sequence of events (Figs. 1a–c) encompassing an axial knee impact involve three main features: knee joint compression, femoral bending and compression, and femoral displacement with load transfer to the hip joint. Each of these facets of response occur at different times in the impact and vary in relative significance. Each may result in a particular mode of injury: knee joint compression may cause patellar or condylar fracture (Fig. 1c), femoral bending may lead to midshaft fracture (Fig. 1a and b), and femoral load transfer may result in femoral neck fracture (not in the field of camera view in this study). Typical kinematics for an axial knee impact with either rigid or lightly padded interface were studied by analysis of high-speed movies to assess knee joint compression during impact. Early in the event the rigid impactor compresses the soft tissue of the knee joint (Fig. 2a). This is followed by a rearward femoral displacement until fracture. In this test the patella, lateral femoral condyle and femoral midshaft were fractured. In the rigid impact tests there was regularly 1.3 cm (Table 2) of

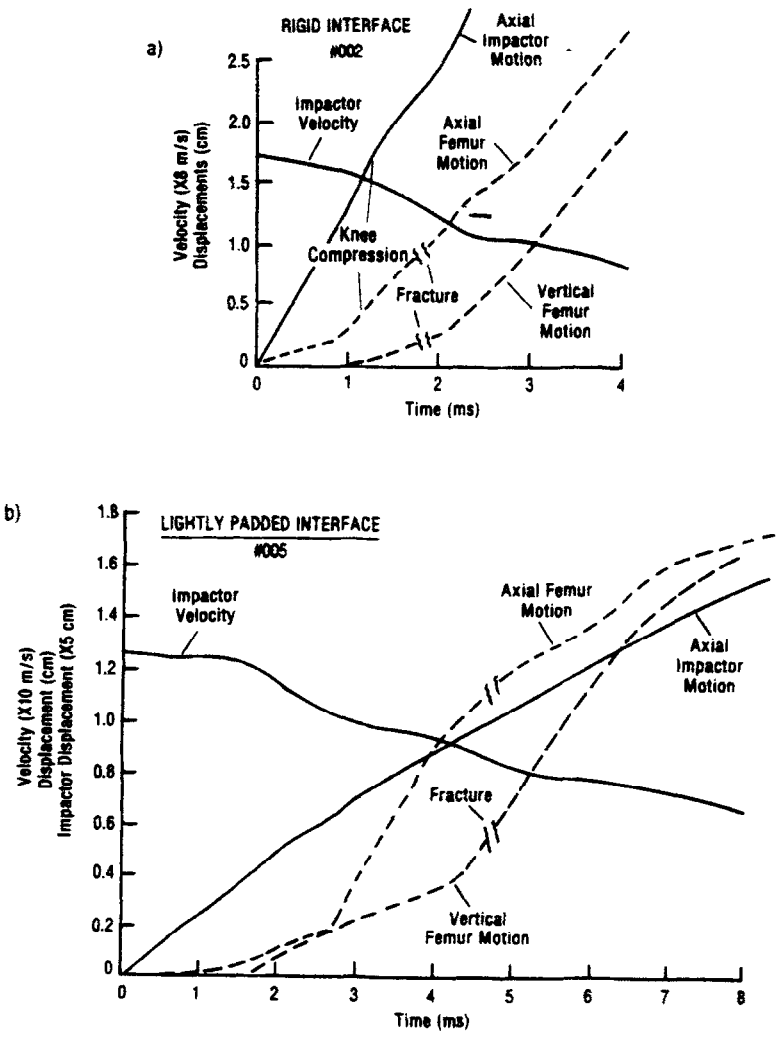

Fig. 2. Analysis of high-speed movies demonstrates the kinematics of impactor motion, femoral displacement and knee-joint compression for (a) rigid (2R20690 A/L) and (b) lightly padded (5LP20698 N/R) impact.

Table 2. Biomechanical and injury responses

Experiments		Kinematics‖,**			Applied forces			Strains††			Skeletal fractures¶			
Test condition*	Impact† velocity (m/s)	Knee-interface compression (cm)	Axial femoral displacement (cm)	Energy transfer (%)	Peak (kN)	Duration (ms)	Fracture‖ (kN)	Occurrence‖ (ms)	Axial compression (%)	Orthogonal bending AP (%/cm)	Orthogonal bending Lateral (%/cm)	Patella	Condyles	Femoral shaft	Neck
1R20690A/R	14.0	1.40	0.97	37	13.5	3.8	13.5	1.83	−0.58	0.49	−0.05	P-Dist-Fx(3)	M-FX(3)	Mid-Fx(3)	
2R20690A/L	14.2	1.21	0.86	50	15.2	3.8	13.2	1.83	−0.08	0.20	−0.13	M-Fx(3)	L-Fx(3)	Mid-Fx(2)	
3R20693N/L	11.4	1.26	0.58	14	13.4	4.4	9.7	1.83				Dist-Fx(3)		Mid-Fx(2)	Fx(2)
4R20693N/R	11.5	1.29	0.97	53	13.4	3.1	9.6	2.83				Dist-Fx(3)		Mid-Fx(2)	Fx(2)
7R20709N/L	14.4	1.32	1.46	70	25.8	3.1	7.0	2.83	−0.62	1.16	−0.02	P-Dist-Fx(3)		Mid-Fx(3)	Fx(2)
8R20709‡N/R	13.6				28.5	4.1						P-Dist-Fx(3)		Mid-Fx(3)	Fx(2)
	13.2 (±1.4)	1.30 (±0.07)	0.97 (±0.32)	45 (±21)	18.3 (±6.9)	3.7 (±0.5)	10.6 (±2.7)	2.23 (±0.55)	−0.43 (±0.30)	0.62 (±0.49)	−0.07 (±0.06)				
5LP20698N/R	13.5	4.01	0.93	59	16.0	5.0	5.9	4.45	−0.02	−0.02	0.35		M-Fx/L-Fx(3)		
6LP20698N/L	13.9	4.38	0.72	54	15.4	5.0	6.4	4.45					M-Fx/L-Fx(3)		
	13.7 (±0.3)	4.20 (±0.26)	0.83 (±0.15)	57 (±4)	15.7 (±0.5)	5.0	6.2 (±0.4)	4.45							
9TP§20703N/R	13.5	[7.06]‡‡	[2.93]‡‡	[75]	5.3	11.9		[10.00]‡‡							
10TP20703N/L	13.4	[5.45]	[1.43]	[57]	14.0	8.1		[6.20]	[0.06]§§	[0.30]§§	[−0.09]§§				
11TP20703N/R	13.5	[5.20]	[2.23]	[58]	13.8	10.3		[7.20]	[0.08]§§	[0.58]	[0.11]				
12TP20711A/R	12.1	3.88	2.32	79	8.7	9.4	8.3	7.33	−0.27	1.11	0.59			Mid-Fx(3)	
13TP20711A/L	12.9	4.40	1.52	60	9.3	6.3	6.7	5.33	−1.26	1.10	−0.66		M-Fx(3)		
	13.0 (±0.6)	4.73 (±0.72)	1.92 (±0.57)	70 (±13)	11.5 (±2.8)	8.5 (±1.8)	7.5 (±1.1)	6.42 (±0.92)	−0.77 (±0.70)	1.11 (±0.01)	−0.04 (±0.88)				

* Refer to Footnote Table 1.
† All tests with 10.1 kg impactor mass.
‡ Soft tissue *in situ*.
§ Test with low crush strength Hexcell – responses excluded from averages.
‖ At the time of skeletal fracture occurrence; obtained by film analysis and comparison of concurrent response levels.

†† Principal strains computed from three mid-shaft strain readings ($\varepsilon_1, \varepsilon_2, \varepsilon_3$)
Sign convention: Positive AP Bending strain implies tension on anterior surface; positive lateral bending strain implies tension on lateral surface; axial tension strains are positive.
‡‡ At maximum knee-interface compression.
§§ At maximum AP bending – no injury occurrence.

¶ Injury code:

L	Lateral
M	Medial
P	Posterior
Dist	Distributed
Fx	Fracture
Mid	Midshaft
( )	AIS

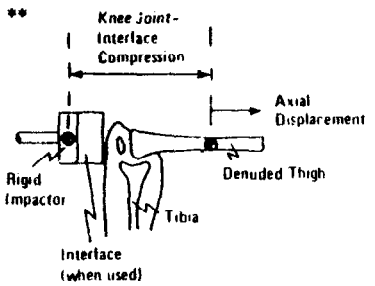

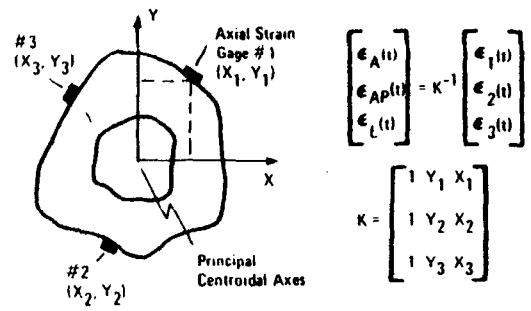

total knee joint compression prior to observed femoral fracture. The padded impacts also produced knee joint compression (Fig. 2b) which was shared by the deformation of the interface. For the lightly padded impacts the maximum compression of 4.20 cm involves at least 1.66 cm of knee-joint compression because of the maximum available interface thickness of 2.54 cm. Other impacts with thickly padded (crushable) material were conducted but the exact extent of joint compression could not be decoupled from the interface response.

As the tissue compresses, the apparent stiffness of the knee joint increases and the femur starts to undergo predominantly axial acceleration and motion. Because of the complex three-dimensional geometry of the femur and its attachment in the hip joint, the distal end of the femur also tended to rise and move laterally under axial impact. The component of axial displacement of the proximal femur shaft was slightly less than 1 cm at fracture for the rigid impacts. Since fracture occurs after only 2 ms of knee contact and nearly 1 cm of femoral displacement, approximately 5 kN of inertial force would be required to square wave accelerate an effective 1 kg femoral–hip joint mass through that distance. Thus, nearly half of the applied force at fracture would be involved in displacing the femur–hip joint mass. This level of axial motion was similar in the lightly padded impacts but increased significantly when a large thickness of padded interface was available. For those impacts where fracture did not occur, responses were tabulated (Table 2) at the moment of maximum knee-interface compression.

In all cases the impactor continuously transfers energy to the 'knee–thigh–hip' complex. For these impacts the slowing of the impactor velocity from contact to fracture initiation was used to compute energy transfer at the time of fracture. The average transfer of energy to the specimen (and interface) increases with the addition of padding. Rigid impact injuries occurred when 45 per cent of the initial available energy of the impactor was transferred to the specimen (i.e., approximately 396 J of the 880 J available kinetic energy). This energy fraction increased to 57 per cent for lightly padded impacts (i.e., 540 J of 948 J available kinetic energy) and to 70 per cent for thickly padded impacts (i.e., 597 J of 853 J available kinetic energy). Naturally the transfer of kinetic energy is through many different mechanisms: energy absorbed or stored in the compression of the knee-joint, energy stored by bending and compression of the femur, energy transferred to accelerating body segments, and energy absorbed by padded interfaces. The energy stored as viscoelastic strain in the tissue and bone is, however, very important since various investigators (Cooke and Nagel, 1969; McElhaney and Byars, 1966; and Yamada and Evans, 1970) have reported limits to the amount of tolerable strain energy in biological tissues.

The time history of the knee joint compression (Fig. 3a and b) indicates a smooth pattern of deformation up to the structural limit of the femur. Bone failure is closely clustered around a knee joint compression state of 1.3 cm for rigid impacts and is more loosely related to the time after contact. The response picture is much more erratic when the history of the applied force is studied (Fig. 3c and d). On the average, the applied load at fracture was 10.6 kN (i.e., 58 per cent of the average peak applied load – Table 2) for the rigid impacts. The peak force occurred from 0.5 ms to 1.5 ms before the initiation of observed femoral fracture. A light and thick padding interface did not significantly affect the temporal difference between peak force and injury initiation. Since the early levels of applied force are partially associated with inertial accelerations which displace coupled masses, it is possible that the peak applied load exceeds the load level at observed fracture. In these tests the peak applied force at fracture did not correlate with the temporal initiation of observed condylar and midshaft fracture or the induced structural deformation of the femur (See Fig. 4a). The occurrence of peak force did seem to coincide with the plateau in knee joint compression.

Average force–deformation curves (Fig. 3e and f) for rigid and lightly padded impacts demonstrate the composite response of knee joint compression and applied force. The average responses for the observed occurrence of the skeletal injury is also shown. The apparent stiffness of the knee joint for moderate states of joint compression seems to be significantly affected by the particular specimen's premortem history, age and skeletal integrity (degree of osteoporosis). Knee joint stiffness averaged 10 kN/cm with a range from 6 kN/cm to 20 kN/cm for the rigid impacts. Since a large variation was observed in the initial linear stiffness of the knee joint and the applied peak force, there is a partial explanation for the relatively constant level of knee joint compression at fracture (i.e., force = stiffness × compression, so that force variability was accounted for by stiffness variability). A similar average 10 kN/cm joint stiffness was observed in the lightly padded impacts when the stiffness computation was taken beyond the point of maximum compression of the interface padding.

Bending and compression strains could be computed up to the initiation of skeletal fracture using the three midshaft uniaxial gage responses and information on the cross-sectional geometry. A typical rigid knee impact response (Fig. 4a) demonstrates a gradual compressive loading of the femur shaft until fracture. Comparison of the strain responses with the applied force history clearly indicates that the peak applied force occurs much earlier than the maximum structural response and fracture of the femur. In this test, the peak applied force occurs after about 1.3 ms of contact exposure. At that point, the knee joint compression is nearly maximum and the femur begins responding as a loaded column. Even though the axial compression increases continuously to failure, the induced anteroposterior (*AP*) femoral bending also increases and

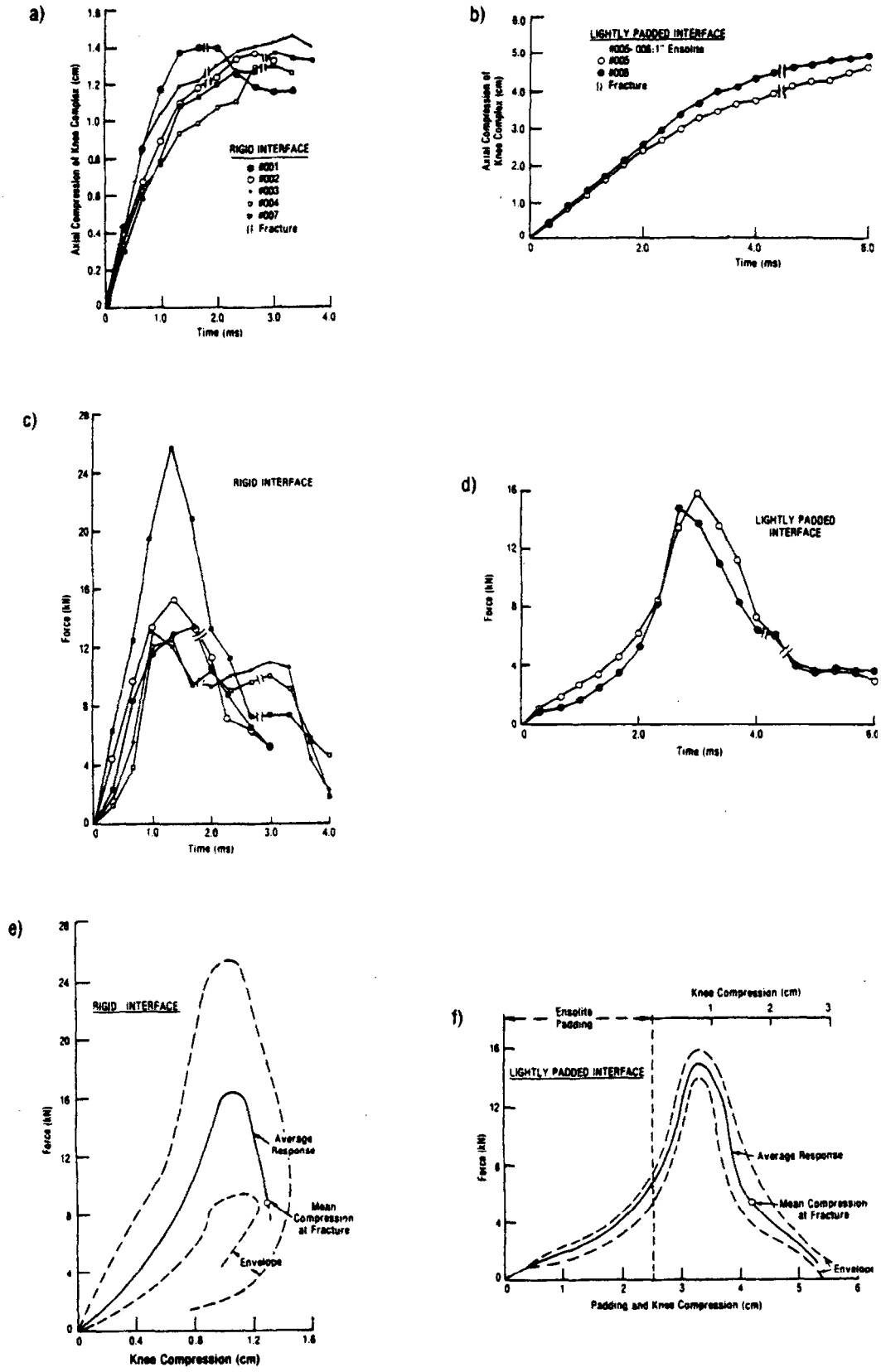

Fig. 3. Biomechanical response of the knee joint compression for dynamic loads applied through the knee to an unrestrained torso. Joint compression increases until fracture; whereas, the applied force reaches a maximum and then decreases before the observed fracture initiates. Composite dynamic force–deformation characteristics of the knee joint are also depicted for a rigid and lightly padded impact.

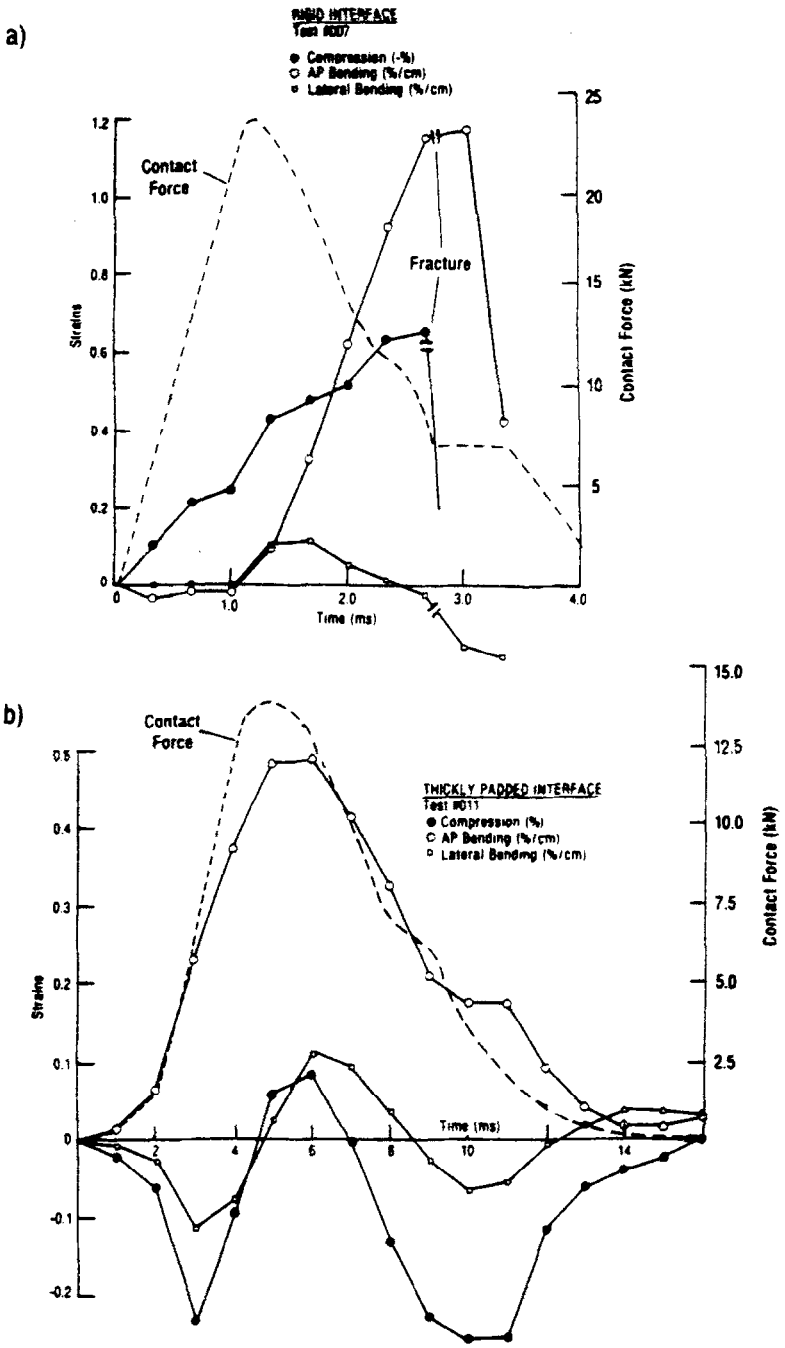

Fig. 4. Anteroposterior and lateral bending and axial compressive strains are shown for a rigid and thickly padded knee impact. (a) Both the level of uniform compression and AP bending increase gradually until fracture. (b) When an injury does not occur, structural vibration in the lateral and axial direction indicates a fundamental frequency of approximately 140 Hz.

becomes the dominant factor associated with the midshaft fracture (Figs. 1a and b). Fracture initiation, which occurs on the anterior midshaft surface, is the result of tension at the site of failure. In this typical example, a tensile strain of 1.22% [1.16%/cm (1.59 cm)–0.62%] was computed at the site of fracture initiation. All midshaft fractures in this experimental study were directly linked to anteroposterior bending which induced tension on the anterior femoral surface exceeding the load-carrying ability of the compact bone (approximately 1.4% tensile strain – Yamada and Evans, 1970). The level of tensile strain on the anterior surface varied considerably with the particular subject in this test series, as did the degree of osteoporosis and skeletal integrity of the cadaver specimens. However, the mechanism of midshaft failure by tensile strain was consistent for all occurrences.

An example of a noninjurious femoral response (Fig.

4b) demonstrates a complicated beam–column impact response (Viano and Khalil, 1976b and 1976c and Viano 1977b). However, the midshaft strain response followed closely the time history of the applied knee load, indicating a much lower component of force inertially accelerating the femur. Various dynamic structural responses are apparent with the natural mode of vibration at about 140 Hz. This is consistent with the range of 100–200 Hz femoral resonant frequencies observed in cadaver and volunteer impedance vibration studies (Melvin and Stalnaker, 1975 and 1976). In the current example, the structural vibration is directed laterally and axially with the *AP* bending predominantly a quasistatic 'column-like' response.

Injuries to the patella and femoral condyles occurred frequently in this test series as well as in previous studies (Lister and Wall, 1970; Melvin and Stalnaker, 1975 and 1976; Powell *et al.*, 1974 and 1975; and Viano, 1977b). Again, observed failures of the femoral condyles seemed to be a direct result of induced tension, either through *AP* bending of the condyles (Fig. 1c lateral view) or lateral–medial wedging by the compressive effects of the patella (Fig. 1c anterior view). The most serious damage of the patella was diffuse comminuted fractures generally emanating from the posterior aspect. In many cases, a lateral and/or medial chip was found displaced in the knee joint at autopsy.

Since direct observation of the femoral neck was not included in the experimental protocol, the sequence of events leading to neck failure is largely conjecture based on circumstantial evidence. The rearward displacement of the femur produces loads in the femoral neck and would be expected to develop tensile strains on the posterior aspect of the femoral neck and hip joint. Femoral neck fracture frequently occurred in rigid impact experiments. Although femoral neck fracture might be suspected of the force dropoff prior to the observed fracture, it is judged to occur moderately late in the event because of: (1) the smooth increasing bending and compressive midshaft strains (Fig. 4a) after the peak in applied force, (2) similar response profiles for rigid and lightly padded impacts with and without neck fracture, (3) the smooth pelvic accelerations beyond peak force (see Stalnaker *et al.*, 1977), and (4) the early component of applied force accelerating the femur and coupled masses distal to the hip joint would not be part of the reaction force at the femoral neck. However, additional tests with a denuded hip joint would be needed for identification of the mechanism and temporal occurrence of femoral neck fracture.

Although the pelvic acceleration responses are not directly addressed in this analysis (see Stalnaker *et al.*, 1977 for raw response data), a few observations seem warranted. The peak pelvic acceleration consistently lags the peak in applied force by 2–5 ms. In some cases the pelvic acceleration peak is contemporaneous with the initiation of the observed femoral fracture, but in other cases it lags the fracture occurrence. Because the back mount was midsagittally positioned high on the iliac spine and only one leg was subjected to impact, the occurrence of the peak response is significantly influenced by angular accelerations. The pelvis appears somewhat loosely coupled to the impact event, due probably to the knee joint compression, structural bending of the femur, and the femoral head deformation in the hip joint, which preceeds the pelvic response.

SUMMARY

In this experimental study, six human cadavers with denuded femurs were subjected to knee impact with a 10.1 kg flat-faced mass with a velocity of 12.1–14.4 m/s. The line of action of the applied force was directed through the femoral axis (axial femoral impact). Analysis of biomechanical and kinematic responses for these tests indicates that:

1. During impact, the knee joint compresses up to a maximum of 1.30 ± 0.07 cm at the initiation of the observed condylar or midshaft fracture. The joint demonstrated an initial linear stiffness of approximately 10 kN/cm. Joint compression can ultimately cause wedging or bending failures of the femoral condyles (see Fig. 1c) as well as comminuted fractures of the patella. However, as the joint compression approaches a maximum, the femur inertially displaces and structurally deforms.

2. The peak in applied load for rigid impacts occurred 0.5 ms to 1.5 ms before the initiation of the observed condylar or midshaft fracture. On the average, the applied knee load at fracture (10.6 ± 2.7 kN) was only 58 per cent of the earlier peak knee load (18.3 ± 6.9 kN). The applied force produces both inertial displacements of the lower extremity and structural deformations of the knee-joint and femur. These reactions occur simultaneously and superimpose in differing proportions during the impact. It appears that a significant portion of the early peak force inertially accelerates the femur and coupled masses, while the remainder develops tolerable deformations in the knee-joint and femur.

3. Maximum compression of the knee joint showed very little variation in level (1.3 ± 0.1 cm, coefficient of variability $CV = 5.4\%$) at the initiation of observed fracture in the rigid impact experiments. This is in contradistinction to larger variations observed in peak applied load ($CV \approx 37.7\%$) and knee load at observed fracture ($CV = 25.5\%$).

4. Strain gages bonded to the femoral midshaft were used to calculate the axial bending strains in orthogonal principle planes (anterior–posterior and lateral–medial) and the uniform state of axial compression. The midfemoral strains up to fracture initiation (see Fig. 4a) indicate that anteroposterior bending gradually increases in significance until it dominates the midshaft response. Eventually, the anterior tensile strain surpasses the load-carrying ability of the com-

pact bone and fracture initiates (see Fig. 1a and b). In these experiments the applied force passes its maximum value while the midshaft bending and compressive strains continue to increase until fracture initiation.

Acknowledgement – We should like to extend our appreciation to Dr. J. W. Melvin and Mr. Guy Nusholtz who assisted in the impact experiments at the Highway Safety Research Institute at the University of Michigan.

REFERENCES

Advani, S. H., Ganga Rao, H. V., Marhia, R. B. and Chang, H. Y. (1975) Structural response of human femurs to axial loads. *Proc. natn. struct. Engng Convention*: American Society of Civil Engineers.

Cooke, F. W. and Nagel, D. A. (1969) Biomechanical analysis of knee impact. *Proc. 13th Stapp Car Crash Conf.* P-28, Society of Automotive Engineers: SAE 690800, 113–117.

Drucker, M. M. and Wynne, G. F. (1975) Avulsion of the posterior cruciate ligament from its femoral attachment: an isolated ligamentous injury. *J. Trauma*, **15**, 616–617.

Goldsmith, W. (1972) *Biomechanics of head injury*. Ch. 23: Biomechanics – its foundations and objectives (Edited by Fung, Y. C., Perrone, N. and Anliker, M.). pp. 585–634, Prentice-Hall, New Jersey.

Horsch, J. D. and Patrick, L. M. (1976) Cadaver and dummy knee impact response. *Soc. Automotive Engineers*, SAE 760799.

Kennedy, J. C. and Fowler, P. J. (1971) Medial and anterior instability of the knee. *J. Bone Jt. Surgery*, **52-A**, 1257–1270.

Kennedy, J. C., Weinberg, H. W. and Wilson, A. S. (1974) The anatomy and function of the anterior cruciate ligament. *J. Bone and Jt. Surg.* **56-A**, 223–235.

King, J. J., William, R. S. and Vargovick, R. J. (1973) Femur load injury Criteria – a realistic approach. *Proc. 17th Stapp Car Crash Conf.*, Society of Automotive Engineers: SAE 760984, 509–524.

Koch, J. C. (1917) The laws of bone architecture. *Am. J. Anat.* **21**, 102, 117–208.

Kramer, M., Burow, K. and Heger, A. (1973) Fracture mechanism of lower legs under impact load. *Proc. 17th Stapp Car Crash Conf.*, Society of Automotive Engineers: SAE 760817, 583–606.

Kroell, C. K., Schneider, D. C. and Nahum, A. M. (1976a) Comparative knee impact response of Part 572 dummy and cadaver subjects. *Proc. 20th Stapp Car Crash Conf.*, Society of Automotive Engineers: SAE 760817, 583–606.

Kroell, C. K. (1976b) Thoracic response to blunt frontal loading. Publication P-67: *The Human Thorax-Anatomy, Injury and Biomechanics*, Society of Automotive Engineers, 49–77.

Kulowski, J. (1964) Fractures of the shaft of the femur resulting from automobile accidents. *J. Int. Coll. Surg.* **42**, 412–420.

Lister, R. D. and Wall, J. G. (1970) Determination of injury threshold levels of car occupants involved in road accidents. *Compendium of the* 1970 *International Automobile Safety Conference*, Society of Automotive Engineers: SAE 700402, 813–833.

McElhaney, J. H. and Byars, E. F. (1966) Dynamic response of biological Materials. *J. appl. Physiol.* **21**,

Melvin, J. W., Stalnaker, R. L., Alem, N. M., Benson, J. B. and Mohan, D. (1975) Impact response and tolerance of the lower extremities. *Proc. 19th Stapp Car Crash Conf.*, Society of Automotive Engineers: SAE 751159, 543–560.

Melvin, J. W. and Stalnaker, R. L. (1976) *Tolerance and response of the knee–femur–pelvis complex to axial impact*. Highway Safety Research Institute Publication: UM-HSRI-76-33, University of Michigan.

Noyes, F. R., Torvik, P. J., Hyde, W. B. and DeLucas, J. L. (1974) Biomechanics of ligament failure – II. An analysis of immobilization, exercise, and reconditioning effects in primates. *J. Bone Jt. Surg.*, **56-A**, 1406–1418.

Noyes, F. R. and Grood, E. S. (1976) The strength of the anterior cruciate ligament in humans and Rhesus monkeys. *J. Bone Jt. Surgery* **58-A**, 1074–1082.

Noyes, F. R. (1977) Functional properties of knee ligaments and alterations induced by immobilization – a correlative biomechanical and histological study in primates. *Clin. Orthop.* **123**, 210–242.

O'Donnel, T. F., Brewster, D. C., Darling, R. C., Veen, H. and Waltman, A. A. (1977) Arterial injuries associated with fractures and/or dislocations of the knee. *J. Trauma* **17**, 775–784.

Patrick, L. M., Kroell, C. K. and Mertz, H. J. (1965) Forces on the human body in simulated crashes. *Proc. 9th Stapp Car Crash Conf.*, Society of Automotive Engineers: 237–260.

Powell, W. R., Advani, S. H., Clark, R. N., Ojala, S. J. and Holt, D. J. (1974) Investigation of femur response to longitudinal impact. *Proc. 18th Stapp Car Crash Conf.*, Society of Automotive Engineers: SAE 741190, 539–556.

Powell, W. R., Ojala, S. J., Advani, S. H. and Martin, R. B. (1975) Cadaver femur responses to longitudinal impacts. *Proc. 19th Stapp Car Crash Conf.*, Society of Automotive Engineers: SAE 751160, 561–580.

Radin, E. L. and Paul, I. L. (1971) Importance of bone in sparing articular cartilage from impact. *Clin. Orthop.* **78**, 342–344.

Radin, E. L., Parker, H. G., Pugh, J. N. *et al.* (1973) Response of joints to impact loading III, relationship to trabecular microfractures and cartilage degeneration. *J. Biomechanics* **6**, 51–57.

Repo, R. U. and Finlay, J. B. (1977) Survival of articular cartilage after controlled impact. *J. Bone Jt. Surg.* **59-A**, 8.

Stalnaker, R. L., Nusholtz, G. S. and Melvin, J. W. (1977) *Femur impact study*. Highway Safety Research Institute Publication: UM-HSRI-77-25, University of Michigan.

Trickey, E. L. (1968) Rupture of the posterior cruciate ligament of the knee. *J. Bone Jt. Surg.* **50B**, 334–342.

Viano, D. C., Helfenstein, U., Anliker, M. and Ruegsegger, P. (1976a) Elastic properties of cortical bone in female human femurs. *J. Biomechanics* **9**, 703–710.

Viano, D. C. and Khalil, T. B. (1976b) Plane strain analysis of a femur midsection. *Proc. 4th New England Bioengng Conf.*, Pergamon Press, 45–48.

Viano, D. C. and Khalil, T. B. (1976c) Investigation of impact response and fracture of the human femur by finite element modeling. *Proc. mathematical modeling biodynamic response to impact* SP-412, Society of Automotive Engineers: SAE 760773, 53–60.

Viano, D. C. (1977a) Considerations for a femur injury criterion. *Proc. 21st Stapp Car Crash Conf.*, Society of Automotive Engineers: SAE 770925, 443–474.

Viano, D. C. (1977b) Experimental investigation of femoral fracture. *Proc. 5th New England Bioengng Conf.*, Pergamon Press, 47–51.

Viano, D. C., Culver, C. C., Haut, R. C., Melvin, J. W., Bender, M. and Levine, R. S. (1978a) Bolster impacts to the knee and tibia of human cadavers and an anthropomorphic dummy. *Proc. 22nd Stapp Car Crash Conf.*, Society of Automotive Engineers, SAE 780890, 167–208.

Viano, D. C. (1978b) Thoracic injury potential. *Proc.* 1978 *Int. Conf. Biokinetics of Impact* (IRCOBI).

Yamada, H. and Evans, F. G. (1970) *Strength of Biological Materials*, Williams and Wilkins, Baltimore, MD.